CORROSION SCIENCE AND TECHNOLOGY, Vol.20, No.1(2021), pp.15~21
[Research Paper]
pISSN: 1598-6462 / eISSN: 2288-6524
DOI: https://doi.org/10.14773/cst.2021.20.1.15

Using Coffee-Derived Hard Carbon as a Cost-Effective and Eco-Friendly Anode Material for Li-Ion Batteries

Sung Joo Hong, Seong Su Kim, and Seunghoon Nam†

Department of Materials Science and Engineering, College of Engineering, Andong National University, 36729 Andong, Gyeongsangbuk-do, Republic of Korea

(Received January 26, 2021; Revised January 27, 2021; Accepted January 27, 2021)

Through a simple filtration process, followed by carbonization within a reductive environment, coffee waste grounds can be transformed into a non-porous hard carbon for use in multiple contexts. This resulting coffee-waste carbon has been evaluated as an eco-friendly and cost-effective replacement for conventional graphite. When compared with different types of carbon, our study found that the coffee-waste carbon fell into the category of hard carbon, as verified from the galvanostatic charge/discharge profiles. The coffee-waste carbon showed a superior rate capability when compared to that of graphite, while compromising smaller capacity at low C rates. During electrochemical reactions, it was also found that the coffee-waste carbon is well exposed to electrolytes, and its disordered characteristic is advantageous for ionic transport which leads to the low tortuosity of Li ions. Finally, the high irreversible capacity (low initial Coulombic efficiency) of the coffee-waste carbon, which if also often observed in amorphous carbon, can be adequately resolved through a solution-based prelithiation process, thereby proving that the coffee-waste carbon material is quite suitable for commercial use as an anode material for quickly-chargeable electrodes.

Keywords: *Coffee waste, Hard carbon, High-rate anodes, Li-ion batteries*

1. Introduction

The emerging sector of electric vehicles (EVs) requires that advances in Li-ion batteries be made for energy storage with higher energy and power densities. Particularly, high-rate charging is much significant to such automotive Li-ion batteries, and the next-generation electrodes must be designed to overcome electronic and ionic transport limitations [1-3]. Furthermore, the cost of Li-ion batteries is also of great concern since Li-ion batteries make up a large portion of the total electric and/or hybrid cars, therefore, the cost reduction of EVs are highly dependent upon the price of Li-ion batteries. The major factor determining the cost of Li-ion batteries is that of the constituent electrode materials, where the current form of Li-ion batteries consists of graphite (natural or artificial) and lithium-transition metal oxides as negative and positive electrodes, respectively.

Despites the changes and improvement on the battery chemistries, graphite is the only commercialized anode materials, and has been adopted for Li-ion batteries for several decades [4-8]. Natural graphite consists of parallel sheets of interconnected hexagons of carbon atoms, and exhibits several advantages including low working potentials (< 0.2 V vs. Li^+/Li), stable cycle-life performance, and reasonable capacity of ~372 mAh/g, overwhelming vast majority of anode materials as Li-alloys, $Li_4Ti_5O_{12}$, transition-metal oxide, etc [9]. However, it is generally accepted that electrodes made of graphite limit the total power density of the whole batteries, due to sluggish Li-ion transport from high tortuosity of graphite electrodes [10]. Synthetic or artificial graphite can be an alternative to such natural graphite in terms of rate capability, while compromising the specific capacity and cost of materials processing [11-13].

It has been reported that naturally-derived carbon can be obtained from various biomasses, and is found to exhibit molecular structures suitable for Li-ion storage and transport in/out of the materials as well as advantages in price [14-16]. Carbons derived from cherry, olive stones, sweet potatoes, mushrooms, and rice husk have been reported for such application. Of naturally occurring carbon precursors, coffee grounds can also be an eco-friendly re-

†Corresponding author: shnam@anu.ac.kr
Sung Joo Hong: M.S Candidates, Seong Su Kim: M.S Candidates, Seunghoon Nam: Professor
S. J. Hong and S. S. Kim contributed equally to this work.

placement for graphite-based electrodes in that global coffee production creates more than ~20 million tons of wastes every year, most of which is discarded in the form of coffee grounds. The use of coffee grounds as sustainable and low-cost anode materials can also be a sensible way of waste and by-product management [17].

In this study, we investigate the possible use of coffee-waste carbon as an optional material for fast-chargeable negative electrode. No activation steps were included in the procedures for preparation of the coffee-derived carbon, and the electrochemical performances of the coffee-waste carbon were evaluated with a half-cell configuration. The resulting low-cost carbon showed superior rate capability to that of natural graphite with stable cycle-life performances. Meanwhile, the enhancement of initial Coulombic efficiency (ICE) of the coffee waste was shown by a solution-based prelithiation, proving possible commercialization of the materials.

2. Experimental Methods

2.1 Fabrication of Coffee-Waste Carbon

The coffee-waste carbon was synthesized by a simple and cost-effective method. Firstly, the coffee-waste grounds were collected from Starbucks. The coffee wastes were mixed and ground with mortar and pestle to exclude the type of coffee beans. The coffee wastes were cleaned with D. I. water and ethanol several times by vacuum filtration prior to carbonization. The homogenized coffee wastes were then heated up to 800 °C for 5 h with a heating rate of 10 °C /min in a quartz-tube furnace.

2.2 Materials Characterization

The morphologies of the coffee-waste carbon were characterized using a scanning electron microscope (FE-SEM, MIRA3 XMH: Tescan). The crystal structure was examined by x-ray diffraction (XRD, D8 Advance: Bruker). In order to analyze the surface chemistry of the coffee-waste carbon, photoelectron spectroscopy (XPS, AXIS-HSi: KRATOS) measurement was conducted. Volumetric N_2 adsorption isotherms (at 7 K) up to 1 bar were measured using a Micromeritics ASAP 020 static volumetric gas adsorption instrument. The specific surface area of the coffee-waste carbon was obtained by the Brunauer-Emmet-Teller (BET) method.

2.3 Electrochemical Characterization

The working electrodes were prepared with active materials, Super P carbon black, and polyvinylidene fluoride binder at a weight ratio of 8:1:1. The slurry was cast on Cu foil, and dried at 110 °C in vacuum overnight. All of the electrodes were assessed in 2032 half-cell configuration with a Li metal as a counter electrode. The loading levels of active material in all of the electrodes was set to be around 1 mg/cm^2. Before the cell assembly, the electrodes were dried under vacuum for 1 h to remove residual water. 1 M $LiPF_6$ in ethylene carbonate (EC), dimethyl carbonate (DMC), and ethylmethyl carbonate (EMC) (1:1:1 vol %) was used as an electrolyte (Panax Etec). Throughout the article, 1 C is defined as 372 mA/g based on the theoretical capacity of single-crystal graphite. The prelithiation was rendered by 0.5 M Lithium-biphenyl complex in tetrahydrofuran (THF). For the chemical prelithiation, the coffee-waste carbon composite electrode was dipped into Li-biphenyl in THF solution for 3 min, and dried in a glove box filled with Ar for 30 min. Cyclic voltammetry (CV) was measured using a potentiostat (Zive MP1:). The CV curves were obtained at a scan rate of 0.01 mV/s.

3. Results and Discussion

3.1 Synthesis and characterization

For the synthesis of coffee-waste carbon, some amount of coffee grounds was collected, and washed several times by vacuum filtration. The obtained coffee grounds were dried at 120 °C in vacuum. Afterwards, the dried powders were carbonized in Ar/H_2 atmosphere for 5 h. With the calcination temperature of 800 °C, the synthetic procedure is quite straightforward, and is cost-effective. The overall procedures for production of the coffee-waste carbon are summarized in the experimental methods.

The powder x-ray diffractions (XRD) patterns of natural graphite and coffee-wasted carbon are shown in Fig. 1a. The overall patterns are similar, apart from the degree of crystallinity. Graphite exhibits sharp and strong peak at ~26° which corresponds to (002) diffraction [18]. Diffraction of the coffee-waste carbon leads to a broad peak at ~23°, only to show short-range order of a typical hard carbon composed of disordered collections of small graphitic grains [19,20]. With (002) diffraction peaks fitted, the peak positions of graphite and coffee-waste are determined, and the resulting *d*-spacings of (002) are calculated to be 3.36 Å and 3.84 Å for graphite and coffee-waste carbon, respectively (insets of Fig. 1a). It is expected that the increased *d* (002) of the coffee-waste carbon facilitates the diffusion of Li^+ in/out of the graphitic layers during battery cycling [21].

The field-emission scanning electron microscopy (FE-SEM) images of Fig. 1b show that the coffee-waste carbon consists of agglomerated particles with interconnected hollow structures. During the thermal calcina-

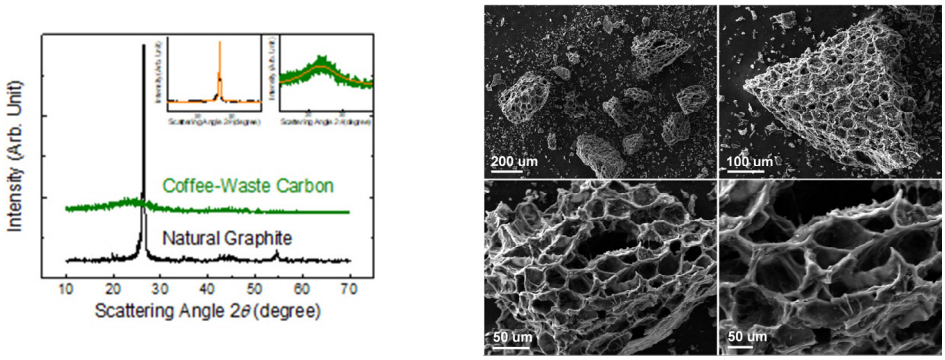

(a) (b)

Fig. 1 (a) XRD patterns of the graphite and coffee-waste carbon. The insets are zoomed-in images with fitted curves (orange lines) using the Voigt function. (b) SEM images of the coffee-waste carbon with different magnifications.

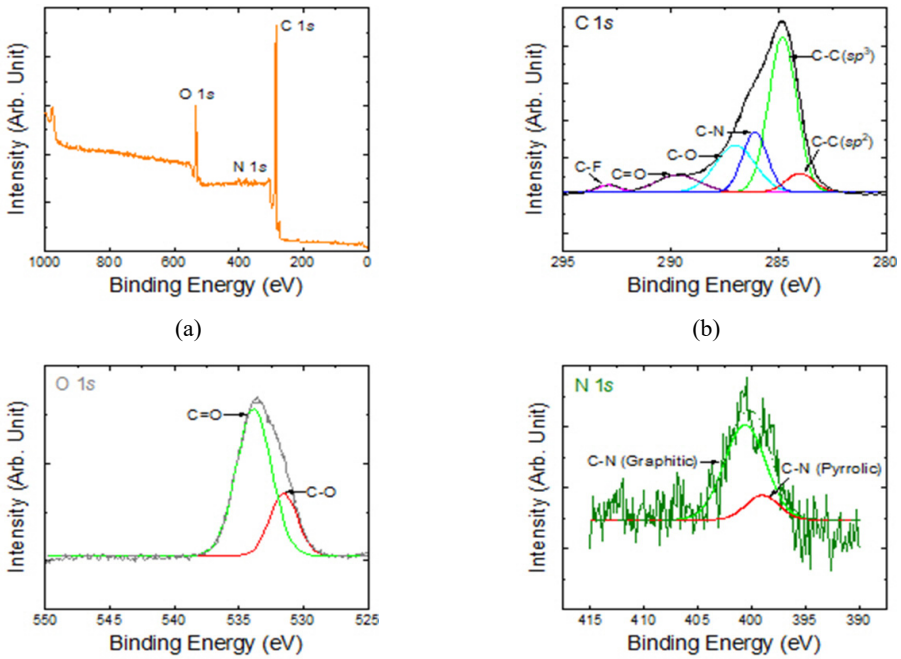

(a) (b)

(c) (d)

Fig. 2 (a) XPS survey spectrum of the coffee-waste carbon. High resolution (b) C 1s, (c) O 1s, (d) N 1s spectra of the coffee-waste carbon. The XPS spectra were fitted to Gaussian functions, and de-convoluted to assign relevant chemical bonds. Each bond is indicated with arrows. The backgrounds were subtracted before the multiple-peak fitting.

tion in a reductive atmosphere, such gases as H_2O, CO, and CO_2 are released through the coffee grounds particles, and the pressure induced by the gas evolutions might have led to the crumbled structure [22]. Obviously, this kind of morphology is advantageous to infiltrate electrolyte inside the structure, which gives rise to rapid Li-ion transport with small tortuosity through the coffee-waste carbon electrode.

Chemical compositions of the coffee-waste carbon were identified by X-ray photoelectron spectroscopy (XPS) in Fig. 2. The survey of spectrum corroborates the presence of carbon, oxygen, and nitrogen at the surface of the coffee-waste carbon (Fig. 2a). Each XPS spectrum was fitted with Gaussian function to assign relevant chemical bonds. In Fig. 2b, deconvolution of the C 1*s* spectrum shows 6 multiple peaks at 284 eV, 284.8 eV, 286.2 eV, 287 eV, 289 eV, and 292 eV attributed to C-C (sp^2), C-C (sp^3), C-N, C-O, C=O, and C-F bonds, respectively [23,24]. It could be seen that a vast majority of C-C bonds in coffee-waste carbon are composed of sp^3 carbon as opposed

to sp^2 carbon, which is indicative of hard carbon. From the O 1*s* spectrum (Fig. 2c), the observed peaks at 531.5 eV and 533 eV correspond to C=O and C-O bonds, showing that coffee-waste carbon still has functional groups at the edge of graphitic layers [24]. The N1*s* spectrum in Fig. 2d can be deconvoluted into two component peaks assigned to pyrrolic-N (399.0 eV) and substitutional or graphitic N (400.6 eV), respectively [25-29]. Both pyrrolic and substitutional N come from the caffeine molecule in the coffee grounds. It is seen that the coffee-waste carbon inherently contains nitrogen-doped region in the molecular structure [30]. Particularly important is the incorporation of graphitic nitrogen atoms which is reported to be an enhancer for electrochemical activity of carbon-based materials.

3.2 Electrochemical Performances

Galvanostatic charge/discharge curves of the coffee-waste carbon are shown in Fig. 3a, where the profiles are presented for the first 5 cycles at 0.1 C (= 37.2 mA/g). With a slanted curvature at 0.8 V, the first discharge (lithiation) gives rise to irreversible capacity of ~550 mAh/g, presumably from the solid-electrolyte interphase (SEI) formation and uncompensated Li^+ storage by functional groups of the coffee-waste carbon [31]. The ICE of the coffee-waste carbon is ~50%. From the fact that surface area of the carbon-waste carbon is negligible (BET surface area: ~8 m^2/g), it is highly likely that the irreversible capacity mainly comes from the adsorbed Li^+ in the vicinity of the functional groups (C-H, C-O, etc.) rather than from consumption of Li due to the formation of SEI layers. After the first cycle, the discharge capacity of the coffee-waste carbon tends to saturate to ~270 mAh/g soon after a few cycles. The coffee-waste carbon displays its shape of profile that is quite different from that of graphite. The discharge profile is downward sloping, indicative of one-phase reaction during which Li^+ is intercalated into the carbon grains in a random manner. The shape of the profile and hysteresis between charge and discharge are typical of a hard carbon, as confirmed by the earlier characterizations [32].

Fig. 3b displays cyclic voltammetry (CV) curves of the coffee-waste carbon. The electrode was scanned at a rate of 0.1 mV/s in the range of 0.01 – 2.0 V (vs. Li^+/Li). From open-circuit voltage of 3.0 V, an appreciable anodic current appears at 0.8 V relevant to decomposition of electrolyte and SEI formation [33-36]. Apparently, the irreversible capacity is reflected as the difference in lithiation charges in the first and second cycles. As for the irreversible capacity, two main contributions are claimed by J.

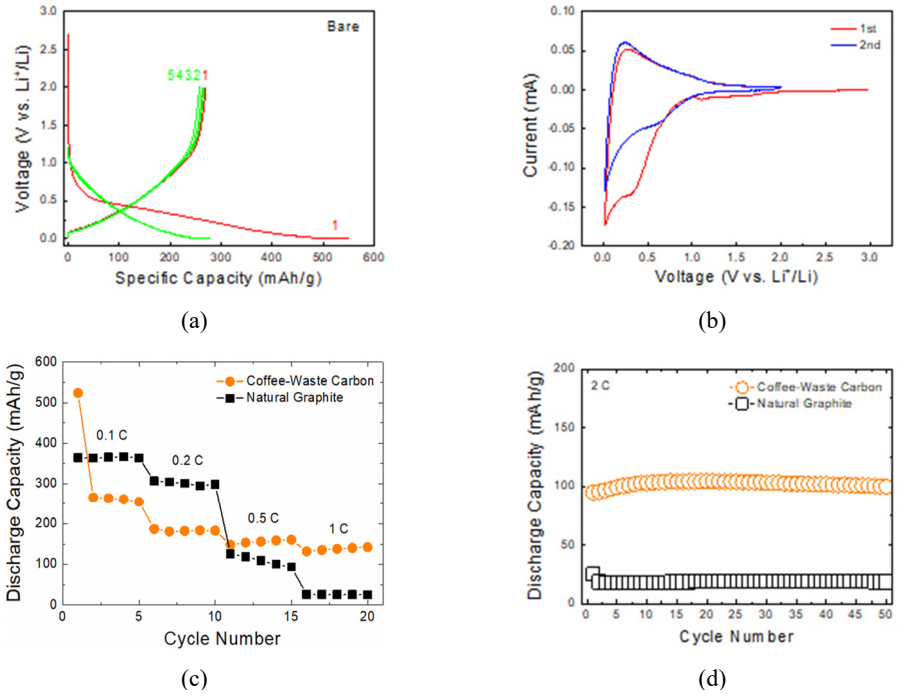

Fig. 3 (a) Voltage profiles of the coffee-waste carbon for the initial 5 cycles at 0.1 C (0.1 C = 37.2 mA/g based upon the theoretical capacity of graphite: 372 mAh/g). (b) Cyclic voltammetry curves of the coffee-waste carbon for the first 2 cycles. (c) Rate capabilities and (d) cycle-life performances (at 2 C) of the coffee-waste carbon and natural graphite.

(a) (b)

Fig. 4 (a) XRD patterns of the graphite and coffee-waste carbon. The insets are zoomed-in images with fitted curves (orange lines) using the Voigt function. (b) SEM images of the coffee-waste carbon with different magnifications.

R. Dahn *et al.*: (1) reaction of Li^+ with electrolyte to form SEI and (2) the reaction of Li^+ with surface functional groups or absorbed entities [37]. Considering surface area of the coffee-waste carbon, the irreversible loss is highly associated with the adsorption of Li^+ in the vicinity of the surface functional groups. The CV curve for the subsequent charge shows a broad cathodic peak corresponding to delithiation from the coffee-waste carbon.

In terms of rate capability (Fig. 3c), the coffee-waste carbon shows less discharge capacities than graphite at 0.1 and 0.2 C. At such a slow rate, the Li insertion kinetics is hardly dependent of the electrode architecture. Instead, the hard carbon retains its moderate capacity at high C rates (0.5 and 1 C), as opposed to natural graphite whose discharge capacity undergoes a sudden decay at 0.5 C and above. It is reported that the rate of charge/discharge is hindered by the limited ion-transport through graphite since insertion/extraction of Li^+ into/out of graphite is highly anisotropic (only in the basal plane of graphene layers) with increased tortuosity of the electrode. In this respect, A. R. Studart *et al.*, magnetically-aligned graphite particles to reduce the tortuosity of thick graphite-based electrode [10]. Moreover, solid-state diffusion of Li^+ within graphite is relatively distant due to the grain size of a few micrometers. In spite of having less reversible capacity than graphite at low C, the coffee-waste carbon, composed of small graphitic grains with turbo-static disorder, is more beneficial for Li^+ diffusion, and undergoes no phase transition and ordering of Li. Hence, such hard carbon as the coffee-waste carbon exhibits higher rate capability than that of the graphite. Increasing the rate up to 2 C makes the differences more notable. As seen in Fig. 3d, the coffee-waste carbon maintains its discharge capacity of ~100 mAh/g for 50 cycles whereas that of the graphite is negligible during cycling.

The irreversible capacity is commonly observed in disordered carbon for battery applications, similar to the coffee-waste carbon. To meet N/P ratios, the uncompensated capacity must be balanced by excessive counter electrode (cathode) materials, while compromising total gravimetric energy density. Reducing the irreversible capacity, thus ICE, is a significant issue with carbon-based materials. Lithiation to anode materials, prior to practical usage, is one of the solutions to tackle the low ICE problem and to pave the way to widespread commercialization [31]. Unlike conventional methods, chemical prelithiation can be rendered by lithium-organic solutions as reductive prelithiation reagents. In this respect, the coffee-waste carbon was prelithiated by Li-biphenyl complex to verify the possible enhancement of ICE. For the prelithiation, an electrode made of the coffee-waste carbon is prepared, and is directly dipped into the Li-biphenyl solution [38,39]. Method of the prelithiation is illustrated in Fig. 4a.

As can be seen in Fig. 4b, the degree of prelithiation can be estimated by lowered open-circuit voltage (OCV) of the coffee-waste carbon since the voltage of electrode are merely a function of Li composition within the electrode material. With the OCV of ~0.5 V, a large portion of the irreversible capacity is vanished indicating that the solution-based prelithiation is achieved. The prelithiation clearly enhances ICE of the coffee-waste carbon electrode nearly up to 96%, as compared to 50% without prelithiation process. It is not likely that the prelithiation adversely affects cycle life of the electrode during the subsequent cycles.

4. Conclusions

A type of carbonaceous materials was synthesized from spent coffee-waste grounds and evaluated as an alternative anode material to conventional graphite. The resulting coffee-waste carbon only required low-cost and eco-friendly synthetic method, and showed better electrochemical performances than the natural graphite. The coffee-waste car-

bon was identified to be a nonporous hard carbon (surface area < 10 m^2/g). The composite electrode made of the coffee-waste carbon showed an excellent rate capability with a reversible capacity of 100 mAh/g at 2 C, while that of the natural graphite underwent severe capacity fading at fast rates. It was also interesting that the chemical prelithiation greatly reduced the irreversible capacity of the coffee-waste carbon, even though the effect of prelithiation on the cyclability and rate should be further investigated. The solution-based prelithiation could be implemented into commercial battery industry where a scalable roll-to-roll process is often adopted. Consequently, the prelithiated coffee-waste carbon could be a commercial replacement for conventional graphite as a fast-chargeable negative electrode.

Acknowledgments

This work was supported by a Research Grant of Andong National University.

References

1. J. Liu, Z. Bao, Y. Cui, E. J. Dufek, J. B. Goodenough, P. Khalifah, Q. Li, B. Y. Liaw, P. Liu, A. Manthiram, Y. S. Meng, V. R. Subramanian, M. F. Toney, V. V. Viswanathan, M. S. Whittingham, J. Xiao, W. Xu, J. Yang, X.-Q. Yang, and J.-G. Zhang, *Nat. Energy*, **4**, 180 (2019). https://doi.org/10.1038/s41560-019-0338-x
2. J. Betz, G. Bieker, P. Meister, T. Placke, M. Winter, and R. Schmuch, *Adv. Energy Mater*., **9**, 1803170 (2019). https://doi.org/10.1002/aenm.201803170
3. Z. Lin, T. Liu, X. Ai, and C. Liang, *Nat. Commun*., **9**, 5262 (2018). https://doi.org/10.1038/s41467-018-07599-8
4. J.-M. Tarascon and M. Armand, *Nature*, **414**, 359 (2001). https://doi.org/10.1038/35104644
5. M. Armand and J.-M. Tarascon, *Nature*, **451**, 652 (2008). https://doi.org/10.1038/451652a
6. B. Scrosati and J. Garche, *J. Power Sources*, **195**, 2419 (2010). https://doi.org/10.1016/j.jpowsour.2009.11.048
7. B. Dunn, H. Kamath, and J.-M. Tarascon, *Science*, **334**, 928 (2011). https://doi.org/10.1126/science.1212741
8. D. Andre, H. Hain, P. Lamp, F. Maglia, and B. Stiaszny, *J. Mater. Chem. A*, **5**, 17174 (2017). https://doi.org/10.1039/C7TA03108D
9. J. Asenbauer, T. Eisenmann, M. Kuenzel, A. Kazzazi, Z. Chen, and D. Bresser, *Sustain. Energy Fuels,* **4**, 5387 (2020). https://doi.org/10.1039/D0SE00175A
10. J. Billaud, F. Bouville, T. Magrini, C. Villevieille, and A. R. Studart, *Nat. Energy*, **1**, 16097 (2016). https://doi.org/10.1038/nenergy.2016.97
11. C. Ma, Y. Zhao, J. Li, Y. Song, J. Shi, Q. Guo, and L. Liu, *Carbon*, **64**, 537 (2013). https://doi.org/10.1016/j.carbon.2013.07.089
12. J. Yue, X. Zhao, and D. Xia, *Electrochem. Commun.*, **18**, 44 (2012). https://doi.org/10.1016/j.elecom.2012.02.001
13. J. Li, Q, Guo, J. Shi, X. Gao, Z. Feng, and Z. Fan, *Carbon*, **50**, 2045 (2012). https://doi.org/10.1016/j.carbon.2011.12.004
14. J. C. Arrebola, A. Caballero, L. Hernan, J. Morales, M. Olivares-Martin, and V. Gomez- Serrano, *J. Electrochem. Soc*., **157**, A791 (2010). https://doi.org/10.1149/1.3425728
15. A. Caballero, L. Hernan, and J. Morales, *ChemSusChem* **4**, 658 (2011). https://doi.org/10.1002/cssc.201000398
16. B. Campbell, R. Ionescu, Z. Favors, C. S. Ozkan, and M. Ozkan, *Sci. Rep*., **5**, 14575 (2015). https://doi.org/10.1038/srep14575
17. J. H. Um, Y. Kim, C.-Y. Ahn, J. Kim, Y.-E. Sung, Y.-H. Cho, S.-S. Kim, and W.-S. Yoon, *J. Electrochem. Sci. Technol*., **9**, 163 (2018). https://doi.org/10.5229/JECST.2018.9.3.163
18. Z. Li, J. Wang, X. Liu, S. Liu, J. Ou, and S. Yang, *J, Mater, Chem*., **21**, 3397 (2011). https://doi.org/10.1039/C0JM02650F
19. J. Shu, M. Shui, D. Xu, S. Gao, X. Li, Y. Ren, L. Hou, J. Cui, J. Xu, and Z. Zhu, *J. Electroanal. Chem*., **657**, 187 (2011). https://doi.org/10.1016/j.jelechem.2011.03.031
20. M. C Shin, J. H Kim, S Nam, Y. J Oh, H.-J Jin, C. R Park, Q. Zhang, and S. J Yang, *Small*, **16**, 2003104 (2020). https://doi.org/10.1002/smll.202003104
21 K Persson, V. A. Sethuraman, L. J. Hardwick, Y. Hinuma, Y. Shirley Meng, A. van der Ven, V. Srinivasan, R. Kostecki, and G. Ceder, *Phys. Chem. Lett.*, **1**, 1176 (2010). https://doi.org/10.1021/jz100188d
22. Y. Oh, S. Nam, S. Wi, J. Kang, T. Hwang, S. Lee, H. H. Park, J. Cabana, C. Kim, and B. Park, *J. Mater. Chem. A* **2**, 2023 (2014). https://doi.org/10.1039/C3TA14347C
23. Y. Liu, L.-Z. Fan, and L. Jiao, *J. Mater. Chem. A*, **5**, 1698 (2017). https://doi.org/10.1039/C6TA09961K

24. K. Krishnamoorthy, M. Veerapandian, K. Yun, and S.-J. Kim, *Carbon*, **53**, 38 (2013). https://doi.org/10.1016/j.carbon.2012.10.013
25. D. C. Wei, Y. Q. Liu, Y. Wang, H. L. Zhang, L. P. Huang, and G. Yu, *Nano Lett*., **9**, 1752 (2009). https://doi.org/10.1021/nl803279t
26. C. P. Ewels and M. Glerup, *J. Nanosci. Nanotechnol*., **5**, 1345 (2005). https://doi.org/10.1166/jnn.2005.304
27. R. J. J. Jansen and H. Vanbekkum, *Carbon*, **33**, 1021 (1995) https://doi.org/10.1016/0008-6223(95)00030-H
28. Y. Nakayama, F. Soeda, and A. Ishitani, *Carbon*, **28**, 21 (1990). https://doi.org/10.1016/0008-6223(90)90088-G
29. J. Casanovas, J. M. Ricart, J. Rubio, F. Illas, and J. M. Jimenez-Mateos, *J. Am. Chem. Soc*., **118**, 8071 (1996). https://doi.org/10.1021/ja960338m
30. L. G. Bulusheva, V. Okotrubab, G. Kurenya, H. Zhang, H. Zhang, X. Chen, and H. Song, Carbon, 49, 4013 (2011). https://doi.org/10.1016/j.carbon.2011.05.043
31. W. Xing, and J. R. Dahn, *J. Electroanal. Chem*., **144**, 1195 (1997) https://doi.org/10.1149/1.1837572
32. X. Rao, Y. Lou, J. Chen, H. Lu, B. Cheng, W. Wang, H. Fang, H. Li, and S. Zhong, *Front. Energy Res*., **8** (2020). https://doi.org/10.3389/fenrg.2020.00003
33. S.Huang, Z. Li, B. Wang, J. Zhang, Z. Peng, R. Qi, J. Wang, and Y. Zhao, *Adv. Funct. Mater.*, **28**, 1706294 (2018). https://doi.org/10.1002/adfm.201706294
34. J. Zhang, H. Zhu, P. Wu, C. Ge, D. Sun, L. Xu, Y. Tang, and Y. Zhou, *Nanoscale,* **7**, 18211 (2015). https://doi.org/10.1039/C5NR05568G
35. W. Tang, B. M. Goh, M. Y. Hu, C. Wan, B. Tian, X. Deng, and C. Peng, M. Lin, J. Z. Hu, and K. P. Loh, *J. Phys. Chem. C,* **120**, 2600 (2016). https://doi.org/10.1021/acs.jpcc.5b12551
36. Y. Li, Y. S. Hu, M. M. Titirici, L. Chen, and X. Huang, *Adv. Energy Mater*., **6**, 1600659 (2016). https://doi.org/10.1002/aenm.201600659
37. E. Buiel and J. R. Dahn, *Electrochim. Acta*, **45**, 121 (1999). https://doi.org/10.1016/S0013-4686(99)00198-X
38. G. Wang, F. Li, D. Liu, D. Zheng, Y. Luo, D. Qu, T. Ding, and D. Qu, *ACS Appl. Mater. Interfaces*, **11**, 8699 (2019). https://doi.org/10.1021/acsami.8b19416
39. X. Zhang, H. Qu, W. Ji, D. Zheng, T. Ding, C. Abegglen, D. Qiu, and D. Qu, *ACS Appl. Mater. Interfaces*, **12**, 11589 (2020). https://doi.org/10.1021/acsami.9b21417